HHS Public Access

Author manuscript

Bioconjug Chem. Author manuscript; available in PMC 2021 September 16.

Published in final edited form as:

Bioconjug Chem. 2020 September 16; 31(9): 2179–2190. doi:10.1021/acs.bioconjchem.0c00365.

Genetic Code Expansion Enables Site-Specific PEGylation of a Human Growth Hormone Receptor Antagonist through Click Chemistry

Kyle Tamshen[1], **Yue Wang**[2], **Stephen M.F. Jamieson**[3,4], **Jo K. Perry**[2,3], **Heather D. Maynard**[1,5,6,*]

[1]Department of Chemistry and Biochemistry, University of California, Los Angeles, California 90095-1569, United States

[2]Liggins Institute, University of Auckland, Auckland 1203, New Zealand

[3]Maurice Wilkins Centre for Molecular Biodiscovery, Auckland 1023, New Zealand

[4]Auckland Cancer Society Research Centre, School of Medical Sciences, University of Auckland, Auckland 1023, New Zealand

[5]California NanoSystems Institute, University of California, Los Angeles, California 90095-1569, United States

[6]Department of Bioengineering, University of California, Los Angeles, California 90095-1569, United States

Abstract

Regulation of human growth hormone (GH) signaling has important applications in the remediation of several diseases including acromegaly and cancer. Growth hormone receptor (GHR) antagonists currently provide the most effective means for suppression of GH signaling. However, these small 22 kDa recombinantly engineered GH analogs exhibit short plasma circulation times. To improve clinical viability, between 4–6 molecules of 5 kDa poly(ethylene glycol) (PEG) are nonspecifically conjugated to the 9 amines of the GHR antagonist designated as B2036 in the FDA-approved therapeutic pegvisomant. PEGylation increases the molecular weight of B2036 and considerably extends its circulation time, but also dramatically reduces its bioactivity, contributing to high dosing requirements and increased cost. As an alternative to nonspecific PEGylation, we report the use of genetic code expansion technology to site-specifically incorporate the unnatural amino acid propargyl tyrosine (pglY) into B2036 with the goal of producing site-specific protein-polymer conjugates. Substitution of tyrosine 35 with pglY yielded a B2036 variant containing an alkyne functional group without compromising bioactivity, as verified by a cellular assay. Subsequent conjugation of 5, 10, and 20 kDa azide-containing PEGs via the copper catalyzed click reaction yielded high purity, site-specific conjugates with

*Correspondence should be addressed to: Heather D. Maynard, Ph.D., 607 Charles E. Young Drive East, University of California, Los Angeles, CA 90095-1569, maynard@chem.ucla.edu.

Supporting Information

The Supporting Information is available free of charge on the ACS Publications website. DNA and protein sequences, NMR spectra, supplementary SDS-PAGE, and supporting MS data.

>89% conjugation efficiencies. Site-specific attachment of PEG to B2036 is associated with substantially improved *in vitro* bioactivity values compared to pegvisomant, with an inverse relationship between polymer size and activity observed. Notably, the B2036–20 kDa PEG conjugate has a comparable molecular weight to pegvisomant, while exhibiting a 12.5 fold improvement in half-maximal inhibitory concentration in GHR-expressing Ba/F3 cells (103.3 nM vs. 1289 nM). We expect that this straightforward route to achieve site-specific GHR antagonists will be useful for GH signal regulation.

Graphical Abstract

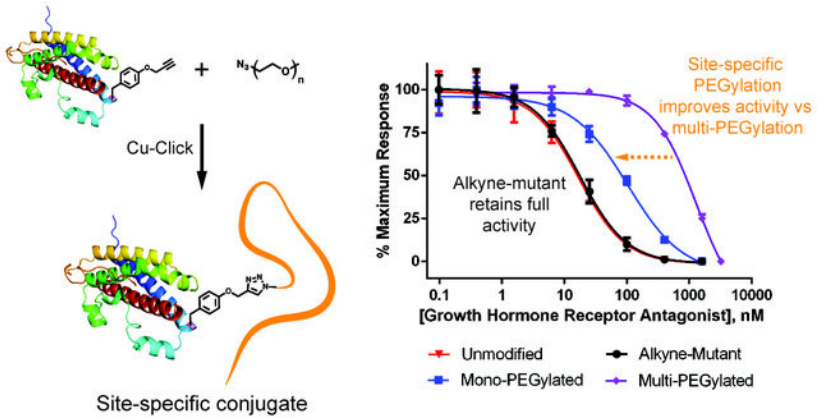

Keywords

growth hormone; GHR antagonist; genetic code expansion; site-specific conjugation; click chemistry; PEGylation

Introduction

Human growth hormone receptor (GHR) antagonists are a class of recombinantly engineered protein therapeutics designed to block human growth hormone (GH) signaling.[1,2] Regulation of GH signaling is important for treatment of acromegaly[3,4] and has also been investigated for use in treatment of GH and insulin-like growth factor 1 (IGF-1)-dependent cancers.[5–9] Acromegaly is a disease characterized by overproduction of GH that can lead to numerous complications if left untreated including diabetes, hypertension, cardiomyopathy, and reduced life expectancy.[3,4] GH signaling also plays a significant role in the development and progression of various cancers, with elevated levels of GH and downstream signaling molecules linked to increased risk of breast cancer, prostate cancer, colon cancer, and others.[4,10–13] In each case, regulation of GH signaling is crucial, and with it, the need for molecules that can most effectively facilitate this regulation.

GH is an important basal pituitary hormone that promotes growth in adolescents and regulates metabolism in adults.[14] Once secreted from the pituitary gland, GH signal transduction occurs upon binding to the GHR located on the surface of cell membranes. Human GH possesses two distinct binding sites that allow it to bind to and promote dimerization of two identical GHR.[15] Following the initial high-affinity binding of one

GHR molecule to GH via binding site 1, GH recruits and facilitates dimerization with a second GHR molecule via its lower-affinity binding site 2.[16] While GH acts as an effective GHR agonist, a single mutation from glycine to lysine at residue 120 in GH binding site 2 transforms the protein into an antagonist. This mutant also binds to and facilitates GHR dimerization, but does not promote signal transduction.[17,18] Since this initial discovery, eight additional mutations have been identified and incorporated to improve GHR binding to GH binding site 1,[1,19] ultimately resulting in the GHR antagonist designated as B2036. As with native GH, B2036 is a small protein of approximately 22 kDa that exhibits rapid blood clearance, with a short half-life in humans of approximately 15 minutes.[20] To extend the half-life of B2036, poly(ethylene glycol) (PEG) with an average molecular weight of 5 kDa was nonspecifically conjugated to 4–6 of the 9 amino groups (8 lysines and the N-terminus) of the protein to generate pegvisomant (Pfizer Inc., USA), which is FDA-approved for acromegaly treatment.

Although multi-PEGylation extended the half-life of B2036 to approximately 74 hours[2,21], its GHR binding and consequent bioactivity were dramatically reduced,[18] likely due to hindered access of the protein to GHR binding sites. This reduction in bioactivity necessitated elevated dosing levels with a recommended dosage range of 10–30 mg injected subcutaneously once daily after a loading dose of 40 mg.[21] While pegvisomant remains an effective treatment for acromegaly, it is also the most expensive treatment option for the disease. Though it is common for protein therapeutics to be expensive, the cost of pegvisomant is particularly high due in part to the high dosing requirements and also likely as a result of the rigorous quality control process that is required for the inherently heterogeneous mixture that results from nonspecific PEGylation.[22,23] One 2009 study applied an economic model to evaluate the cost-effectiveness of pegvisomant treatment compared to standard care and estimated the cost-effectiveness ratio to be approximately £212,000 per life year gained over a 20 year period. The authors ruled that despite the effectiveness of the drug, it could not be deemed good value for its cost compared to standard care.[24] Reduction of the economic burden of pegvisomant is therefore highly desirable.

One strategy with potential to overcome these barriers is to employ site-specific conjugation of PEG to B2036. Controlled attachment of PEG to specific residues distal to the GHR binding regions can reduce blockage of these sites and facilitate improved bioactivity compared to nonspecific PEGylation. Site-specific protein conjugation strategies are well known and have been reviewed extensively.[25–29] Canonical amino acids within a native protein can be functionalized using a variety of chemical modification strategies, but frequently these methods require extensive optimization to target single residues, and often lack positional specificity in the protein sequence. For example, alkylation of the N-terminal amino group of a protein via reductive amination can be carried out selectively around pH 5 even in the presence of lysine amino groups due to the slight difference in pK_a values between the two types of amino groups. However, competing lysine modification and incomplete protein modification are often observed when employing reductive amination, ultimately diminishing conjugate yields. This approach was used for mono-PEGylation of the N-terminal amino group of B2036 with 20 kDa and 40 kDa PEG chains. Interestingly

only the 20 kDa B2036 conjugate demonstrated *in vivo* bioactivity, which the authors speculated to be a result of interference by the larger PEG with GHR binding sites.[30]

Another approach to install a specific reactive site is to express a recombinant protein containing a genetically incorporated cysteine residue. The resulting nucleophilic thiol can be selectively modified with a variety of commercially available reagents such as maleimides or other Michael acceptors.[31] Though these reactions are quite robust and high yielding, expression and purification of the thiol-containing protein can be challenging due to the potential for oxidation of the installed thiol, which can lead to misfolding and dimerization.[27,32] Addition of reducing agents such as dithiothreitol (DTT) or tris(2-carboxyethyl)phosphine (TCEP) have been used to reverse dimerization, but these reagents can lead to global disulfide reduction or disulfide shuffling, which can interfere with protein function and diminish overall conjugate yields.[27,32,29] Nevertheless, this robust approach remains a mainstay in the field of protein engineering, and several groups, including ours, have reported the preparation of GH and B2036 variants that have demonstrated equivalent bioactivities compared to their native protein using T3C[33] and S144C[34] mutations, respectively. As expected, PEGylation of these variants also led to substantial improvements in bioactivity over the multi-PEGylated pegvisomant.

In more recent years, advances in the field of genetic code expansion have provided alternative opportunities for site-specific protein modifications. Like genetic cysteine incorporation, these amino acids can be substituted into any position in the amino acid sequence, but offer dozens of possible functional handles that can be tailored to meet the specific requirements of a given system. Amber suppression is one of the most common techniques used to site-specifically incorporate unnatural amino acids (UAA) into proteins; it functions by using an amino-acyl tRNA synthetase/tRNA pair that is orthogonal to the host organism's translational machinery, but can effectively be recognized by the host ribosome and facilitate reassignment of the amber-stop codon to a particular UAA.[35] This technique has recently been applied to many proteins including GH to enable site-specific PEGylation. For instance, Cho et al. used amber suppression to prepare twenty site-specifically PEGylated GH variants for receptor binding and evaluated six of the most promising (Y35, F92, Q131, R134, Y143, and K145) for bioactivity, pharmacokinetics, and *in vivo* performance, ultimately identifying tyrosine 35 (Y35) to be the overall best performing PEGylation site.[36] In another report from Wu et al., combinatorial, site-specific PEGylation was explored for three residue positions (Y35, G131, and K145). The authors found that site-specific multi-PEGylated GH variants yielded similar bioactivity as singly-PEGylated GH variants of the same molecular weight, with the multi-PEGylated conjugates additionally exhibiting improved half-lives.[37] While incorporation of multiple UAAs is an attractive option for site-specific multi-PEGylation, it must be noted that presently amber suppression is inherently less efficient than recoding with canonical amino acids. This results in dramatically reduced yield of full-length protein as more amber codons are added to a protein sequence.[35] Similar to cysteine mutants, protein function must also always be reevaluated following UAA incorporation. Yet, incorporation of artificial amino acids has distinct advantages including orthogonally, and while GH has received significant attention for site-specific PEGylation using genetic code expansion as described above, GHR antagonists such as B2036 have not been extensively investigated.

In the work described herein, we developed a robust, user-friendly platform for preparation of a site-specifically PEGylated GHR antagonist with improved cellular bioactivity compared to pegvisomant. We envisioned that a B2036 variant of equal potency could be prepared in good yield without extensive chromatographic purification by incorporation of the noncanonical amino acid propargyl tyrosine in a region of the protein distal to both GHR binding sites. Reaction of the alkyne-containing protein with azide-containing PEGs via the copper catalyzed cycloaddition reaction efficiently yielded single-polymer conjugates that could be purified by simple anion-exchange chromatography. We evaluated the *in vitro* bioactivity of the resulting conjugates and found each to be significantly more potent than pegvisomant, even at comparable molecular weights. Taken together, this work provides a useful strategy for the preparation of site-specific, bioactive, PEGylated GHR antagonists.

Results and Discussion

Design and Preparation of a Site-Specifically Modified GHR Antagonist

There are many parameters to consider when using genetic code expansion to site-specifically install an UAA into a protein of interest. First and foremost is the determination of which UAA to use. One of our primary objectives was to generate a B2036 variant that could be selectively PEGylated at a single residue under mild conditions. Additionally, we sought to use a highly efficient and straightforward conjugation strategy with synthetically accessible reagents, allowing for rapid production of usable protein and conjugates. We also wanted to ensure that the UAA of choice could be incorporated into B2036 with good efficiency in order to obtain usable quantities of the full-length protein. For these reasons, we chose to use propargyl tyrosine (pglY) since its alkyne can react selectively with azides under mild, copper-catalyzed conditions,[38,39] and both pglY and azide-containing reagents can be purchased or prepared with synthetic ease. Furthermore, pglY incorporation relies on the *Methanococcus jannashii* derived amino-acyl tRNA synthetase/cognate amber-suppressing tRNA pair, which is both well established and efficient.[40,41]

Nearly as important as the selection of an UAA is the decision of where to install it. We initially evaluated the reported crystal structure obtained of GH binding with two GHR and identified residues distal to both binding regions.[15] Next, we identified amino acids that were structurally similar to pglY such as tyrosine and phenylalanine so as to minimize structural perturbations following incorporation. Finally, we compared our candidates with literature reports of genetic code expansion applied to structurally similar GH[36,37] and theorized that substitution of tyrosine 35 (Y35) with pglY in GHR antagonist B2036 would provide the most promising candidate (Figure 1).

Expression and purification of B2036 and B2036 Y35pglY (B2036-Alkyne) were then carried out. DNA sequences coding for the mature form of both proteins were genetically fused to an N-terminal tag composed of thioredoxin (TRX) with a hepta-histidine sequence similar to our previously reported construct to promote soluble expression as well as affinity purification.[42] A tobacco etch virus (TEV) protease recognition sequence was engineered between the TRX-His7 tag and the B2036 sequence for eventual removal of the TRX-His7 tag (Figures S3–S6). Plasmids for each fusion construct were transformed into *E. coli* Origami B (DE3) competent cells, a strain engineered to help facilitate soluble

protein expression. Genetic code expansion machinery was encoded by the previously reported plasmid pDule2-CNF,[40] which was co-transformed only with the B2036-Alkyne expression vector. To ensure that this machinery was selective for pglY incorporation, control expressions were assessed with and without the addition of pglY to the growth medium by sodium dodecyl sulfate polyacrylamide gel electrophoresis (SDS-PAGE) (Figure 2A). In the absence of pglY, only a 15 kDa truncation product was observed in the crude cell lysate after induction with isopropyl-β-D-thiogalactopyranoside (IPTG), which corresponds to the expected size of the fusion protein if the amber codon was not suppressed and instead read as a stop codon. In the presence of pglY, a full-length expression band is observed at approximately 33 kDa. Notably, even in the presence of pglY, a significant amount of truncation product was still observed. This is because the cellular machinery used to facilitate incorporation of UAAs is most commonly adapted from other organisms. Imperfect synergy of this non-native machinery with the host cell's translational machinery results in diminished UAA incorporation efficiencies, a byproduct of which is the expression of truncated protein. No observable expression products were observed at 33 kDa in the absence of IPTG.

The fusion protein TRX-B2036-Alkyne was then purified via immobilized metal affinity chromatography (IMAC). As expected, the 15 kDa truncation product, which contained a hepta-histidine tag, bound to and eluted from the Ni-NTA affinity column with the full-length fusion protein (Figure 2B). However, following digestion of the fusion protein with Tobacco Etch Virus (TEV) protease and purification with inverse-IMAC and centrifugal filtration, all byproducts were successfully removed, yielding highly pure B2036-Alkyne (Figure 2C). Following TEV digestion, a single N-terminal glycine residue was added to the amino acid sequence of B2036-Alkyne; however, this small change was not expected to perturb structure or activity as our previously reported construct contained a similar, short N-terminal sequence.[42] Expression was approximately 65% efficient for production of B2036-Alkyne compared to B2036 with yields of 8.7 and 13.3 mg/g cell pellet, respectively. Part of this disparity is due to the noted limitations of the adapted machinery, but some portion can also be attributed to the increased metabolic burden associated with the two-plasmid system used to express B2036-Alkyne versus the single-plasmid system for B2036. For our purposes, we found this yield to be satisfactory as approximately 19 mg of high purity B2036-Alkyne could be purified from each liter of growth media.

Evaluation of Structure and *In Vitro* Bioactivity

Having prepared the pure, putative GHR antagonists, we proceeded to confirm the respective sequences of each as well as the incorporation of pglY into the protein by mass spectrometry (MS). We first validated the molecular weight of the proteins via intact MS analysis and found the deconvoluted masses to match the calculated values (Figure 3A and Figure S7A). We next performed peptide-mapping experiments to confirm the amino acid sequence of each protein and to ensure the site-selectivity of pglY incorporation. Digestion of the pure protein samples with MS-grade trypsin produced peptide fragments that were analyzed by liquid chromatography tandem MS (LC-MS/MS) analysis. Analysis of B2036-Alkyne yielded sequence coverage of 88.5% with coverage for all but the N and C terminal peptide fragments (Figure 3B). Importantly, the desired incorporation of pglY in place of tyrosine

35 was confirmed in this experiment as evidenced by the sample tandem mass spectrum of the peptide fragment from residues 18–39 (Figure 3C and Table S1). A similar analysis was performed for B2036 and 100% sequence coverage was observed (Figure S7B). Taken together, these results confirmed the composition and sequence of each GHR antagonist.

Following structural validation, we next evaluated the bioactivity of each protein to ensure that the addition of pglY into B2036-Alkyne did not perturb its function. Bioactivity was assessed in a resazurin cell viability assay using GH-dependent Ba/F3 cells expressing human GHR developed by the Waters Lab (University of Queensland, St. Lucia, Australia); addition of GHR antagonists blocks GH present in the growth media from binding to GHR and consequently inhibits cellular proliferation in this cell line.[43] By administering serially diluted samples of the antagonists, we generated dose-response curves and determined the half-maximal inhibitory concentration (IC_{50}) for B2036 and B2036-Alkyne to be 16.8 and 17.7 nM, respectively (Figure 4). Statistical analysis revealed no significant difference between these values, showing that incorporation of pglY was not deleterious to GHR binding. Having successfully prepared a GHR-antagonist with a nondisruptive, site-specific reaction handle, we next investigated the amenability of B2036-Alkyne to PEGylation and how attachment of a single polymer would affect bioactivity compared to multi-PEGylation.

Site-Specific PEGylation and Evaluation of Conjugate Bioactivity

We elected to install pglY into B2036 due to the orthogonality, reaction efficiency, and synthetic accessibility of both the alkyne-containing functional group, as well as azide-containing reaction partners. PEG-azides of 5 and 10 kDa were easily prepared in two steps from commercially available methoxy-terminated PEG (mPEG) and the 20 kDa mPEG-azide was purchased. Activation of the terminal alcohol was facilitated by reaction with *p*-toluenesulfonyl chloride in >90% yield, and the azide-terminated mPEG (mPEG-azide) was accessed via subsequent reaction with sodium azide in 78–89% yield. Conjugation of mPEG-azides was carried out starting from well-established procedures for the copper catalyzed azide-alkyne cycloaddition (CuAAC) reaction.[44] However, even when using high-efficiency conjugation reactions such as CuAAC, coupling two macromolecules often requires some level of optimization. To determine the best conditions for high-efficiency PEGylation of B2036-Alkyne, we varied reaction time, copper concentration, and molar equivalents of PEG-azide. Reaction time had little to no apparent effect on conjugation efficiency for times greater than 2 hours, nor did concentration of copper above a threshold of 0.2 mM (data not shown). Interestingly, the reaction proceeded very slowly below this copper threshold, which was similar to a previous report.[45] Notably, the presence of copper was required for conjugations to proceed, indirectly confirming the site-specificity of the conjugation reaction. Adjustment of the molar ratio of PEG-azide proved critical for reaching high conjugation efficiencies, and for 20 kDa mPEG-azide we found that addition of 10 molar equivalents was necessary to reach a reaction conversion of about 90% (Figure S8); addition of extra equivalents failed to further improve conversion.

For this study, we conjugated mPEG-azides of 5, 10, and 20 kDa to B2036-Alkyne via our optimized CuAAC conditions (Figure 5A). The reactions were carried out at 20 °C for 2 hours in 100 mM phosphate buffer, pH 7.0 with 0.45 mM B2036-Alkyne,

4.53 mM mPEG-azide, 0.2 mM copper sulfate ($CuSO_4$), 1 mM ligand (2-(4-((Bis((1-(*tert*-butyl)-1*H*-1,2,3-triazol-4-yl)methyl)amino)methyl)-1*H*-1,2,3-triazol-1-yl)acetic acid, or BTTAA), 5 mM aminoguanidine hydrochloride, and 5 mM sodium ascorbate (Figure 5A). SDS-PAGE analysis of the crude reaction mixtures revealed that each conjugation proceeded to high conversion and the products were already largely pure with only PEG and minimal unreacted B2036-Alkyne remaining (Figure S9). The crude conjugates were easily purified with good peak separation using anion exchange chromatography followed by centrifugal filtration (10 kDa MWCO) of the pooled B2036-PEG fractions to concentrate and remove any remaining small molecules (Figure S10). Endotoxin levels were determined to be <0.25 endotoxin units (EU)/mg for conjugates and unmodified protein, which is well below the recommended dosing limit of <5 EU/mg.[46] Purified conjugates were analyzed by SDS-PAGE stained with Coomassie Brilliant Blue to confirm protein purity and also with 0.1 N iodine solution to confirm removal of excess polymer (Figure 5B & 5C). Addition of 5, 10, and 20 kDa PEGs to B2036 (22 kDa) would give expected conjugate molecular weights of 27, 32, and 44 kDa, respectively. However, the apparent molecular weights of the conjugates by SDS-PAGE were slightly inflated likely due to the large hydrodynamic radius of PEG, with observed molecular weights of approximately 30, 35, and 50 kDa, respectively. Only one higher molecular weight band was observed for each conjugation reaction, confirming the site-specificity of this approach.

Purified site-specifically PEGylated B2036 conjugates were then evaluated for bioactivity in Ba/F3-GHR cells and compared to pegvisomant and B2036-Alkyne. IC_{50} values were found to be 17.7, 54.0, 68.8, 103.3, and 1289 nM for B2036-Alkyne, B2036–5k mPEG, B2036–10k mPEG, B2036–20k mPEG, and pegvisomant, respectively (Figure 6). These results emphasize the relationship between polymer size and bioactivity, as IC_{50} values increased with conjugation of larger polymers to B2036. Despite the reduction in bioactivity following PEGylation, the B2036–20 kDa mPEG conjugate (~42 kDa) demonstrated only 5.8-fold attenuation of bioactivity compared to a 72.8-fold reduction for multi-PEGylated pegvisomant of similar molecular weight (~42–52 kDa). This difference in IC_{50} cannot fully be explained by the slight differences in molecular weight between the two conjugates, but was rather a result of the specificity of the PEG attachment site.

We expect that this site-specifically PEGylated B2036 variant will be of significant interest to researchers investigating GH regulation because it offers a number of advantages. First, the incorporation of pglY into B2036 not only retains the protein activity, but also provides access to the highly specific and orthogonal CuAAC click reaction. Neither azides nor alkynes are cross-reactive with other canonical amino acid functional groups, ensuring that only one polymer can be conjugated to each protein. Additionally, azides and alkynes are stable to the conditions used for protein bioconjugation and these reactions demonstrate excellent conjugation efficiency.[47] This chemistry therefore offers an advantage over other methods where the nucleophile or electrophile is unstable in the aqueous conditions (such as succinimidyl esters). Furthermore, the resultant triazole is stable under biological conditions, whereas certain chemistries are not; for example thiol-maleimide linkages have demonstrated reversibility and may undergo retro-Michael reactions, although this issue has largely been addressed through the design of improved linkers.[47–50] The implementation of CuAAC as the conjugation chemistry also allows B2036-Alkyne to be conjugated to a broad

variety of polymers, fluorophores, positron emission tomography probes, or any other azide-containing compound, many of which are either commercially available or synthetically accessible. Accordingly, this work illustrates the value of rational design coupled with click chemistry in the development of modular, site-specific protein-polymer conjugates.

An additional advantage conferred by this approach is the ability to tune the bioactivity of B2036 via modulation of polymer size. In this study, we observed an inverse relationship between polymer molecular weight and bioactivity. As the size of the polymer conjugated to B2036-Alkyne increases, so does its ability to block access to GHR binding sites, consequently reducing the observed bioactivity of the conjugate. Reduced bioactivity may also result from attenuated binding kinetics of B2036 to GHR due to polymer interference. We expect that a combination of these factors is likely responsible for lowering bioactivity for conjugates with larger conjugated polymers. Previous reports have also noted that conjugation of larger PEGs to GH or B2036 tended to reduce bioactivity compared to the unmodified protein, even for site-specific conjugates.[30,36,37,51] Since proteins tend to exhibit longer circulation times with higher molecular weight PEGs, an inverse relationship between bioactivity and half-life as a function of polymer size is also likely, and has been evidenced with B2036.[30] We therefore expect that our conjugation strategy will be useful in exploring this balance between half-life and bioactivity since the molecular weight of the conjugate can be precisely tuned through addition of a single PEG.

Perhaps most importantly, these site-specific conjugates demonstrated significant improvement of bioactivity compared to the multi-PEGylated pegvisomant. This substantial improvement in bioactivity could contribute to reducing dosing requirements and consequently could help alleviate a portion of the economic burden associated with pegvisomant. Even with the diminished expression yield of B2036-Alkyne of 65% compared to native B2036, we expect the observed 12.5-fold improvement in activity of B2036–20 kDa mPEG over pegvisomant to sufficiently offset this cost. Generally, 65% incorporation efficiency of an unnatural amino acid is relatively high; for example, GH mutants containing a similar unnatural amino acid were prepared in titers ranging from 20–70% compared to the wild type protein depending on the incorporation site.[36] In addition to retaining bioactivity, incorporation of pglY in place of tyrosine 35 also provides B2036-Alkyne in good yield. With these promising results, it must also be acknowledged that improved bioactivity alone is insufficient to reduce dosing regimens if the protein therapeutic is rapidly cleared *in vivo*. Future studies will therefore need to be carried out to determine serum stability and pharmacokinetic parameters for these site-specific conjugates, and these studies are planned in our groups. We expect that the homogeneity of our conjugates as well as the ability to directly modulate protein activity with polymer size will greatly aid efforts toward this research.

Conclusions

In this work, we report the use of genetic code expansion to prepare a mutant of the GHR antagonist B2036 containing a single alkyne-functionalized residue in a region of the protein distal to its GHR binding domains. This mutation did not affect the bioactivity of B2036 in Ba/F3-GHR cells and facilitated site-specific PEGylation, which demonstrated

substantial improvement in bioactivity over the nonspecifically PEGylated pegvisomant. We also established an inverse relationship between the molecular weight of the attached polymer and *in vitro* conjugate bioactivity, which is helpful information for future work focused on balancing bioactivity with pharmacokinetics. Taken together, we expect that our use of rational design and genetic code expansion to generate site-specific protein-polymer conjugates will be of significant interest to others working in the area of GH regulation.

Materials and Methods

Materials

All chemicals and bioreagents were purchased from Sigma-Aldrich or Fisher Scientific and used as received unless otherwise noted. 20 kDa mPEG-azide was purchased from Jenkem USA and 5 kDa and 10 kDa mPEG were purchased from Sigma-Aldrich and used as received. Boc-L-tyrosine methyl ester was purchased from ChemImpex and used as received. BTTAA was purchased from Click Chemistry Tools and used as received. Dichloromethane (DCM) was distilled over CaH_2 and stored under argon. Tetrahydrofuran (THF) was distilled over sodium/benzophenone and stored under argon. Mouse Ba/F3 cells stably expressing human GHR (Ba/F3-GHR) were obtained from Professor Michael Waters (University of Queensland, Australia). Ba/F3-GHR cells were cultured at 37°C with 5% CO_2 in RPMI 1640 media (Gibco RPMI 1640 with L-glutamine, 25 mM HEPES buffer), 5% Fetal Bovine Serum (FBS), 100 U/ml penicillin, 100 μg/ml streptomycin, 1% Glutamax, and 25 ng/ml recombinant human GH. Cells were generally subcultured every three days and split 1:10 into new media. Recombinant human GH was purchased from Dr. A.F. Parlow at the National Hormone and Peptide Program (Harbor-UCLA Medical Center, Torrance, CA) and was resuspended in PBS to 0.5 mg/ml. TEV protease was prepared based on the reported procedure.[52] Plasmids for expression of B2036 fusion constructs were designed by the authors; then the DNA was synthesized and cloned into pET21a expression vectors by Twist Biosciences. The plasmid containing the expanded genetic code machinery for incorporation of propargyl tyrosine via amber suppression was provided by Ryan Mehl (Oregon State University, Corvallis, OR) and is designated as pDule2-CNF (Addgene plasmid #85495).

Analytical Techniques

NMR spectra were obtained on Bruker AV 500 and AV 600 MHz spectrometers with a relaxation delay of 4 seconds for both proton and carbon experiments. Infrared absorption spectra were obtained using a PerkinElmer FT-IR equipped with an attenuated total reflectance (ATR) accessory. High-resolution mass spectra were obtained for small molecules using a Waters Acquity LCT Premier XE equipped with an autosampler and direct injection port. High-resolution mass spectra and peptide mapping were acquired using a Thermo Q Exactive Plus Orbitrap Mass Spectrometer equipped with a direct injection port and switchable UltiMate 3000 nanoLC. Peptide masses were analyzed using Thermo-Fisher Proteome Discoverer software version 1.4. SDS-PAGE was performed using Bio-Rad Any kD Mini-PROTEAN-TGX gels and gels were stained with Coomassie for visualization of protein or 0.1 N iodine for visualization of PEG. SDS-PAGE protein standards were obtained from Bio-Rad (Precision Plus Protein Pre-stained Standards).

Methods

Plasmid Design—Plasmids were designed based on the previously reported construct[42] for the soluble expression of B2036 as a N-terminally tagged thioredoxin (TRX) fusion protein. For this work, a similar construct was engineered to contain an N-terminal TRX-His7-TEV solubility-enhancing, protease-cleavable tag that was then genetically fused to a codon optimized cDNA sequence encoding B2036 (Figures S1–S3). To generate a propargyl tyrosine containing B2036 variant (B2036-Alkyne), the amber codon TAG was inserted into the sequence in place of the DNA encoding residue 35 of the original B2036 protein (Figures S4–S6). Each of these sequences was synthesized and inserted into a pET21a expression vector via restriction cloning between *Bgl*II and *Xho*I sites by Twist Biosciences. These two plasmids were designated pET21a-TRX-B2036 and pET21a-TRX-B2036-Y35TAG for expression of B2036 and B2036-Alkyne, respectively. All plasmid sequences were verified by Sanger sequencing (Eurofins Genomics).

Expression of B2036 and B2036-Alkyne—Plasmids pET21a-TRX-B2036 and pET21a-TRX-B2036-Y35TAG were each transformed into *E. coli* Origami B (DE3) competent cells according to the manufacturer's protocol (Novagen). Plasmid pDule2-CNF, which constitutively expresses an amber-codon suppressing tyrosyl tRNA synthetase and cognate tRNA,[40] was co-transformed with plasmid pET21a-TRX-B2036-Y35TAG in order to provide the genetic code expansion machinery necessary for incorporation of propargyl tyrosine. 5 ml of a saturated overnight culture of each transformant was used to inoculate 1 L of sterile LB medium in a 2.5 L baffled flask containing 50 μg/ml ampicillin for the single plasmid system (pET21a-TRX-B2036) or 50 μg/ml ampicillin and 50 μg/ml spectinomycin for the two-plasmid system (pET21a-TRX-B2036-Y35TAG and pDule2-CNF). Cells were grown at 37°C with shaking at 250 rpm to an OD_{600} of 0.4, at which point protein expression was induced with IPTG to a final concentration of 0.1 mM. For the two-plasmid system, propargyl tyrosine was added to a final concentration of 1 mM simultaneous to IPTG addition. Following induction, cells were grown at 18 °C with shaking at 210 rpm for 20 hours then harvested by centrifugation for 15 min at 5,500 g (6,000 rpm; Beckman JA-14 rotor) and stored at −80°C. Prior to lysis, cells were thawed and resuspended in 30 ml lysis buffer consisting of PBS, pH 7.4 with 150 mM NaCl, 1% Triton X-100, 10% glycerol, and 3 cOmplete Mini Protease Inhibitor Cocktail tablets (Roche). Cell lysis was then carried out by passing cells through an Avestin Emulsiflex C-3 homogenizer two times at 1240 bar with cooling. Crude cell lysates were then clarified via centrifugation for 60 min at 48,300 g (20,000 rpm; Beckman JA-25.50 rotor) and the supernatant was collected for purification.

Purification of B2036 and B2036-Alkyne—Purification was carried out identically for both B2036 and B2036-Alkyne fusion proteins. Supernatant containing protein was filtered through a 0.45 μM syringe filter and then incubated with 5 ml of Ni-NTA resin at 4°C with gentle rocking for 30 min. The supernatant Ni-NTA slurry was then poured into a gravity column and the flow through was poured back over the column twice to maximize binding. The resin was then washed with 6 column volumes (CV) wash buffer 1 (PBS, pH 7.4, with 150 mM NaCl, 10 mM imidazole, 0.1% Triton X-100, and 10% glycerol), then with 4 CV of wash buffer 2 (PBS, pH 7.4 with 150 mM NaCl, 20 mM imidazole, and 10% glycerol), then the column was eluted with 5 CV elution buffer (PBS, pH 7.4 with 150 mM NaCl,

200 mM imidazole, and 10% glycerol). Fractions were analyzed by SDS-PAGE, and pure fusion protein fractions were combined and buffer exchanged by centrifugal filtration with 30 kDa MW filters into PBS, pH 7.4 with 150 mM NaCl and 10% glycerol. Cleavage of the TRX-His7-TEV tag was then facilitated by incubation of the purified fusion proteins with TEV protease (100:1 mass ratio) for 18 hours at 4°C. The digested TRX-His7-TEV tag was then removed via reverse Ni-NTA affinity chromatography. Column flow through was collected and pure protein fractions were combined and concentrated by centrifugal filtration with 10 kDa MW filters. Protein concentration was measured using bicinchoninic acid (BCA) assay (Pierce) and protein purity was assessed by SDS-PAGE.

Intact Mass Analysis and Peptide Mapping Analysis—Purified B2036 and B2036-Alkyne were analyzed by intact mass spectrometry and peptide mapping using a Thermo Q Exactive Plus Orbitrap Mass Spectrometer equipped with a direct injection port and switchable UltiMate 3000 nanoLC. For intact mass spectrometry, purified protein samples were desalted by dialyzing overnight against MilliQ ultrapure water, then filtered through 0.22 μM syringe filters, and the masses were determined following continuous direct sample injection at 50 μl/min using an auxilary syringe pump with acquisition over 30 s. Mass deconvolution was performed using the instrument software. To obtain peptide fragments of the purified proteins for peptide mapping, trypsin digests were performed according to the manufacturer's protocol using MS grade trypsin protease (Pierce). Following digestions, samples were desalted and prepared for analysis as previously reported using Empore stage-tips.[53] Following elution from stage-tips, samples were dried using a speed vac then resuspended in 100 μl 0.5% formic acid in ultrapure water to 0.2 μg/μl. 1.0 μl of each sample was injected onto the spectrometer after first passing through an UltiMate 3000 nanoLC equipped with a 75 μm x 2 cm Acclaim PepMap 100 trap column packed with C18 3 μm bulk resins (Thermo Scientific) and a 75 μm x 15 cm Acclaim PepMap RSLC analytical column packed with C18 2 μm resin (Thermo Scientific) using a method of 3–35% Mobile Phase B over 40 min, then 35–85% Mobile Phase B over 5 min (Mobile Phase A: H_2O with 0.1% formic acid; Mobile Phase B: acetonitrile with 0.1% formic acid; 0.3 μl/min). The spectrometer ESI voltage was set to 1.9 kV with a capillary temperature of 275°C. Full spectra from m/z 350 – 2000 were acquired in profile mode with resolution 70,000 at m/z 200 with an automated gain control (AGC) target of 3×10^6. The most abundant 15 ions were further fragmented by higher-energy collisional dissociation (HCD) with a normalized collisional energy of 25. MS/MS spectra were acquired in centroid mode with resolution 17,500 at m/z 200. The AGC target for fragment ions are set at 2×10^4 with maximum injection time of 50 ms. Dynamic exclusion was set at 45.0 s. The resultant raw data was then analyzed using Proteome Discoverer software version 1.4 (Thermo Scientific) by searching against a subset of the uniprot human database modified to contain the expected protein sequence using the following parameters: precursor mass tolerance was set to ± 10 ppm, fragment mass tolerance was set to ± 0.02 Th for HCD, false discovery rate was set to 1.0%, up to 2 trypsin miscleavages were allowed, a minimum of 1 peptide was required for protein identification, and variable modifications were set to include methionine oxidation and tyrosine propargylation.

PEGylation of B2036-Alkyne—PEGylation of B2036-Alkyne was carried out according to standard copper-catalyzed azide-alkyne click chemistry conditions.[44] All stock solutions were prepared using 100 mM phosphate buffer and this buffer was added to the reaction solution to achieve a final protein concentration of 1 mg/ml. General procedure: In a 1.5 ml conical tube was added 1 mg (261.1 μl; 3.83 mg/ml stock) B2036-Alkyne, 10 molar equivalents of either 5, 10, or 20 kDa mPEG-azide (113 μl, 226 μl, or 453 μl of a 20 mg/ml stock, respectively), and enough 100 mM phosphate buffer to reach a final reaction volume of 1 ml once all remaining components had been added. Next, a $CuSO_4$ stock solution (20 mM) was premixed with a BTTAA ligand stock solution (50 mM) in a 1:2 ratio of $CuSO_4$:BTTAA before a 30 μl aliquot of this premixed solution was added to the B2036-Alkyne solution to a final concentration of 0.2 mM $CuSO_4$ and 1 mM BTTAA. Aminoguanidine hydrochloride was then added to the reaction solution to a final concentration of 5 mM (50 μl; 100 mM stock). Finally, sodium ascorbate was added to the reaction solution to a final concentration of 5 mM (50 μl; 100 mM stock) and the conical tube was sealed and rocked gently at 20 °C for 2 hours. Reactions were monitored by SDS-PAGE and stained with Coomassie to visualize protein and with 0.1 M iodine to visualize PEG. Conjugates were purified and analyzed by FPLC on a Bio-Rad BioLogic DuoFlow chromatography system equipped with a 1 mL GE Healthcare HiTrap Q HP column using a method of 0 to 1 M NaCl in 10 mM PB, pH 7.4, 10% glycerol (Buffer A: 10 mM PB, pH 7.4, 10% glycerol; Buffer B: 10 mM PB, pH 7.4, 10% glycerol + 1 M NaCl; 0.5 mL/min; 1 mg/0.25 mL injections; 4 CV 0% Buffer B, then 8 CV 0–100% linear gradient Buffer B, then 2 CV 100% Buffer B). Concentration of PEGylated B2036 was determined via BCA assay and protein purity was assessed by SDS-PAGE. Endotoxin levels were measured for all proteins and conjugates using a Pierce LAL Chromogenic Endotoxin Quantification Kit following the manufacturer's recommendations.

Cell Viability Assay—Ba/F3-GHR cells were serum starved for 16 h, then plated at 20,000 cells per well (80 μl) in 5% serum media in the interior wells of a Corning Costar 96-well plate; outer wells were filled with sterile water or media to prevent edge effects. 10 μl of serial dilutions of B2036 variants and conjugates in assay media were added to cells to final protein concentrations ranging from 0–1,600 nM, and cells were incubated at ambient temperature for 20 min (n=6 replicates per condition). Next, 10 μl of GH solution was added to each well to a final concentration of 20 ng/ml, and cells were incubated at 37 °C with 5% CO_2 for 48 hours. Cell viability was determined by addition of 5 μl resazurin sodium salt (0.5 mg/ml) to each well followed by incubation at 37 °C with 5% CO_2 for 2 hours. Fluorescence measurements were recorded using a Tecan Infinite M1000 Pro automated plate reader system with an excitation wavelength of 560 nm and an emission wavelength of 590 nm. Statistical analysis and non-linear regression analysis of the resulting values were analyzed using GraphPad Prism software version 6.01. Data is expressed as means with 95% CI and data sets were compared using Student's t-test or one-way ANOVA with post-hoc analyses (Tukey's multiple comparisons test) as necessary. *In vitro* assays were repeated at least two times with a representative figure shown. A p-value of <0.05 was used to determine statistical significance. Half-maximal inhibitory concentration (IC_{50}) values of each antagonist were determined by fitting a sigmoidal dose-response model "log (agonist) vs. response-variable slope (four parameters)."

Synthesis of 5 kDa mPEG-Tosylate—To an oven-dried 50 ml 2-neck round bottom flask equipped with a stir bar, septum, and gas adapter was added 20 ml of dichloromethane (DCM) and 5 kDa mPEG (1.000 g, 0.20 mmol, 1 equiv). Once dissolved, tosyl chloride (0.191 g, 1.00 mmol, 5 equiv) was added followed by dropwise addition of triethylamine (0.139 ml, 1.00 mmol, 5 equiv) and the reaction was stirred at 20°C for 19 h. Anhydrous K_2CO_3 was then added to the reaction and allowed to stir for 10 min before filtering the reaction and concentration under vacuum to a light tan oil. This oil was diluted with minimal DCM and precipitated three times into diethyl ether to yield a white solid (0.945 g, 91.7% yield). See Supporting Information Figure S11 for assigned ^{1}H NMR (500 MHz, $CDCl_3$): δ 7.79 (d, *J* = 8.0 Hz, 2H), 7.33 (d, *J* = 8.3 Hz, 2H), 4.15 (t, *J* = 4.9 Hz, 2H), 3.64 (m, 537H), 3.37 (s, 3H), 2.44 (s, 3H).

Synthesis of 10 kDa mPEG-Tosylate—To an oven-dried 25 ml 2-neck round bottom flask equipped with a stir bar, septum, and gas adapter was added 10 ml of DCM and 10 kDa mPEG (0.500 g, 0.05 mmol, 1 equiv). Once dissolved, tosyl chloride (0.095 g, 0.50 mmol, 10 equiv) was added followed by dropwise addition of triethylamine (0.070 ml, 0.50 mmol, 10 equiv) and the reaction was stirred at 20°C for 24 h. Anhydrous K_2CO_3 was then added to the reaction and allowed to stir for 10 min before filtering the reaction and concentration under vacuum to a light tan oil. This oil was diluted with minimal DCM and precipitated three times into diethyl ether to yield a white solid (0.461 g, 90.8% yield). See Supporting Information Figure S12 for assigned ^{1}H NMR (500 MHz, $CDCl_3$): δ 7.78 (d, *J* = 8.3 Hz, 2H), 7.32 (d, *J* = 8.0 Hz, 2H), 4.14 (t, *J* = 4.9 Hz, 2H), 3.63 (m, 537H), 3.36 (s, 3H), 2.43 (s, 3H).

Synthesis of 5 kDa mPEG-Azide—To an oven-dried 2-neck 25 ml round bottom flask equipped with a stir bar, glass stopper, and condenser was added 10 ml of ethanol followed by 5 kDa mPEG-Tosylate (0.500 g, 0.10 mmol, 1 equiv) and sodium azide (0.033 g, 0.50 mmol, 5 equiv). The mixture was heated to 80 °C in an oil bath for 15 h then removed from heat and allowed to cool to room temperature before concentrating the solution under vacuum. The crude material was then dissolved in ethyl acetate and washed twice with water, then the aqueous layer was extracted 3 times with DCM and the combined organics were dried over anhydrous magnesium sulfate and dried under vacuum to yield a colorless oil. This oil was then diluted with minimal DCM and precipitated in diethyl ether 3 times to yield a white solid (0.388 g, 77.7% yield). See Supporting Information Figure S13 for assigned ^{1}H NMR (500 MHz, $CDCl_3$): δ 3.63 (m, 527H), 3.38 (t, *J* = 5.4 Hz, 2H), 3.37 (s, 3H).

Synthesis of 10 kDa mPEG-Azide—To an oven-dried 2-neck 25 ml round bottom flask equipped with a stir bar, glass stopper, and condenser was added 10 ml of ethanol followed by 10 kDa mPEG-Tosylate (0.100 g, 0.01 mmol, 1 equiv) and sodium azide (0.007 g, 0.10 mmol, 10 equiv). The mixture was heated to 80 °C in an oil bath for 19 h then removed from heat and allowed to cool to room temperature before concentrating the solution under vacuum. The crude material was then partitioned between DCM and water and the organic layer was collected. The aqueous layer was then extracted 3 times with DCM and the combined organics were dried over anhydrous magnesium sulfate and dried under vacuum to

yield a colorless oil. This oil was then diluted with minimal DCM and precipitated in diethyl ether 3 times to yield a white solid (0.088 g, 89.4% yield). See Supporting Information Figure S14 for assigned ^{1}H NMR (600 MHz, $CDCl_3$): δ 3.64 (m, 927H), 3.39 (t, J = 5.1 Hz, 2H), 3.38 (s, 3H).

Synthesis of Boc-L-Propargyl Tyrosine Methyl Ester—To an oven dried 1-neck 100 ml round bottom flask equipped with a stir bar and water condenser was added Boc-L-tyrosine methyl ester (2.000 g, 6.77 mmol, 1 equiv), anhydrous K_2CO_3 (2.808 g, 20.32 mmol, 3 equiv) and 40 ml acetone. The reaction was stirred for several minutes before dropwise addition of propargyl bromide (2.998 ml of 80% solution in toluene, 20.32 mmol, 3 equiv) at ambient temperature. The reaction was then refluxed (72°C) for 23 hours. After cooling to ambient temperature, the reaction was concentrated under vacuum then partitioned between DCM and water and the organic layer was collected. The aqueous layer was extracted 3 times with DCM. The combined organics were dried over anhydrous magnesium sulfate, filtered, and concentrated under vacuum. The resulting crude oil was then purified via silica flash column chromatography using a Biotage Isolera One system equipped with a 50 g SNAP KP-Sil cartridge using a method of 5–40% ethyl acetate in hexane and a flow rate of 100 ml/min (R_f = 0.29; 4:1 hexane:ethyl acetate). Fractions containing the desired product were combined and concentrated under vacuum to give an orange oil (yield determined following deprotection steps). See Supporting Information Figure S15 for assigned ^{1}H NMR (500 MHz, $CDCl_3$): δ 7.01 (d, J = 8.5 Hz, 2H), 6.85 (d, J = 8.7 Hz, 2H), 5.01 (d, J = 8.1 Hz, 1H), 4.61 (d, J = 2.5 Hz, 2H), 4.50 (q, J = 6.6 Hz, 1H), 3.66 (s, 3H), 3.02 (dd, J_1 = 13.9 Hz, J_2 = 5.7 Hz, 1H), 2.94 (dd, J_1 = 13.9 Hz, J_2 = 6.2 Hz, 1H), 2.49 (t, J = 2.4 Hz, 1H), 1.37 (s, 9H). See Supporting Information Figure S16 for assigned ^{13}C NMR (125 MHz, $CDCl_3$): δ 172.4, 156.6, 155.1, 130.3, 129.0, 114.9, 79.8, 78.6, 75.6, 55.8, 54.5, 52.2, 37.4, 28.3. FT-IR: ν 3434, 3386, 3305, 2980, 2935, 2871, 2123, 1738, 1708. HRMS: $C_{18}H_{23}NO_5$ calc. $[M+H]^+$ = 356.1474 Da; obsd. $[M+H]^+$ = 356.1473 Da.

Synthesis of L-Propargyl Tyrosine—Boc-L-propargyl tyrosine methyl ester was dissolved in a mixture of aqueous 1 M NaOH (4 ml) and acetonitrile (4 ml) and stirred for 16 hours at ambient temperature. The solution was then diluted with water, neutralized with citric acid, and extracted 3 times with DCM. The combined organics were dried over anhydrous magnesium sulfate, filtered, and dried under vacuum to yield an orange oil that was immediately taken into the next step. The orange oil was dissolved in 10 ml 45:45:5:5 DCM:TFA:H_2O:TIPS in a 20 ml glass vial and stirred for approximately 10 min before concentrating the solution under vacuum. Once concentrated, the remaining viscous liquid was precipitated twice into 1:1 hexane:diethyl ether to yield a white solid (1.039 g, 70.0% yield over 2 steps) that was determined to be >98% pure by analytical HPLC (Figure S19) and >96% pure by ^{1}H NMR. See Supporting Information Figure S17 for assigned ^{1}H NMR (500 MHz, D_2O): δ 7.15 (d, J = 8.6 Hz, 2H), 6.94 (d, J = 8.6 Hz, 2H), 4.68 (s, 2H), 3.84 (dd, J_1 = 7.7 Hz, J_2 = 5.2 Hz, 1H), 3.11 (dd, J_1 = 14.7 Hz, J_2 = 5.2 Hz, 1H), 2.96 (dd, J_1 = 14.7 Hz, J_2 = 7.8 Hz, 1H), 2.82 (t, J = 2.2 Hz, 1H). See Supporting Information Figure S18 for assigned ^{13}C NMR (125 MHz, D_2O): δ 173.8, 156.1, 130.6, 128.5, 115.6, 78.7, 76.6, 56.0,

56.0, 35.4. FT-IR: ν 3296, 2997, 2964, 2922, 2866, 2135, 1611, 1555, 1512 cm^{-1}. HRMS: $C_{12}H_{13}NO_3$ calc. $[M+H]^+$ = 220.0974 Da; obsd. $[M+H]^+$ = 220.0932 Da.

Supplementary Material

Refer to Web version on PubMed Central for supplementary material.

Acknowledgements

This work was funded by the National Institutes of Health (NIBIB R01EB020676). The authors thank Prof. Michael Waters (University of Queensland, St. Lucia, Australia) for the Ba/F3-GHR cell line, Prof. Ryan Mehl (Oregon State University, Corvallis, OR) for the pDule2-CNF plasmid, Neil Forsythe (University of California, Los Angeles, CA) for TEV protease, Dr. Yu Chen (University of California, Los Angeles, CA) for technical assistance with mass spectrometry analysis, and Dr. Mark Arbing (University of California, Los Angeles, CA) for helpful discussions on protein expression.

References

(1). Kopchick JJ; Parkinson C; Stevens EC; Trainer PJ (2002) Growth Hormone Receptor Antagonists: Discovery, Development, and Use in Patients with Acromegaly. Endocr. Rev. 23, 623–646. [PubMed: 12372843]

(2). Muller AF; Kopchick JJ; Flyvbjerg A; van der Lely AJ (2004) Growth Hormone Receptor Antagonists. J. Clin. Endocrinol. Metab. 89, 1503–1511. [PubMed: 15070905]

(3). Colao A; Grasso LFS; Giustina A; Melmed S; Chanson P; Pereira AM; Pivonello R (2019) Acromegaly. Nat. Rev. Dis. Primer 5, 1–17.

(4). Renehan AG; Brennan BM (2008) Acromegaly, Growth Hormone and Cancer Risk. Best Pract. Res. Clin. Endocrinol. Metab. 22, 639–657. [PubMed: 18971124]

(5). McCutcheon IE; Flyvbjerg A; Hill H; Li J; Bennett WF; Scarlett JA; Friend KE (2001) Antitumor Activity of the Growth Hormone Receptor Antagonist Pegvisomant against Human Meningiomas in Nude Mice. J. Neurosurg. 94, 487–492. [PubMed: 11235955]

(6). Dagnaes-Hansen F; Duan H; Rasmussen LM; Friend KE; Flyvbjerg A (2004) Growth Hormone Receptor Antagonist Administration Inhibits Growth of Human Colorectal Carcinoma in Nude Mice. Anticancer Res. 24, 3735–3742. [PubMed: 15736405]

(7). Divisova J; Kuiatse I; Lazard Z; Weiss H; Vreeland F; Hadsell DL; Schiff R; Osborne CK; Lee AV (2006) The Growth Hormone Receptor Antagonist Pegvisomant Blocks Both Mammary Gland Development and MCF-7 Breast Cancer Xenograft Growth. Breast Cancer Res. Treat. 98, 315–327. [PubMed: 16541323]

(8). Yin D; Vreeland F; Schaaf LJ; Millham R; Duncan BA; Sharma A (2007) Clinical Pharmacodynamic Effects of the Growth Hormone Receptor Antagonist Pegvisomant: Implications for Cancer Therapy. Clin. Cancer Res. 13, 1000–1009. [PubMed: 17289896]

(9). Evans A; Jamieson SMF; Liu D-X; Wilson WR; Perry JK (2016) Growth Hormone Receptor Antagonism Suppresses Tumour Regrowth after Radiotherapy in an Endometrial Cancer Xenograft Model. Cancer Lett. 379, 117–123. [PubMed: 27241667]

(10). Jenkins PJ; Mukherjee A; Shalet SM (2006) Does Growth Hormone Cause Cancer? Clin. Endocrinol. (Oxf.) 64, 115–121. [PubMed: 16430706]

(11). Guevara-Aguirre J; Balasubramanian P; Guevara-Aguirre M; Wei M; Madia F; Cheng C-W; Hwang D; Martin-Montalvo A; Saavedra J; Ingles S; et al. (2011) Growth Hormone Receptor Deficiency Is Associated with a Major Reduction in Pro-Aging Signaling, Cancer, and Diabetes in Humans. Sci. Transl. Med. 3, 70ra13–70ra13.

(12). Chhabra Y; Waters MJ; Brooks AJ (2011) Role of the Growth Hormone–IGF-1 Axis in Cancer. Expert Rev. Endocrinol. Metab. 6, 71–84. [PubMed: 30764037]

(13). Subramani R; Nandy SB; Pedroza DA; Lakshmanaswamy R (2017) Role of Growth Hormone in Breast Cancer. Endocrinology 158, 1543–1555. [PubMed: 28379395]

(14). Olarescu NC; Gunawardane K; Hansen TK; Møller N; Jørgensen JOL Normal Physiology of Growth Hormone in Adults. In Endotext; Feingold KR; Anawalt B; Boyce A; Chrousos G; Dungan K; Grossman A; Hershman JM; Kaltsas G; Koch C; Kopp P; et al. Eds.; MDText.com, Inc.: South Dartmouth (MA), 2000.

(15). de Vos A; Ultsch M; Kossiakoff AA (1992) Human Growth Hormone and Extracellular Domain of Its Receptor: Crystal Structure of the Complex. Science 255, 306–312. [PubMed: 1549776]

(16). Pradhananga S; Wilkinson I; Ross RJM (2002) Pegvisomant: Structure and Function. J. Mol. Endocrinol. 29, 11–14. [PubMed: 12200225]

(17). Fuh G; Cunningham BC; Fukunaga R; Nagata S; Goeddel DV; Wells JA (1992) Rational Design of Potent Antagonists to the Human Growth Hormone Receptor. Science 256, 1677–1680. [PubMed: 1535167]

(18). Ross RJM; Leung KC; Maamra M; Bennett W; Doyle N; Waters MJ; Ho KKY (2001) Binding and Functional Studies with the Growth Hormone Receptor Antagonist, B2036-PEG (Pegvisomant), Reveal Effects of Pegylation and Evidence That It Binds to a Receptor Dimer. J. Clin. Endocrinol. Metab. 86, 1716–1723. [PubMed: 11297608]

(19). Cunningham BC; Wells JA (1989) High-Resolution Epitope Mapping of HGH-Receptor Interactions by Alanine-Scanning Mutagenesis. Science 244, 1081–1085. [PubMed: 2471267]

(20). Veldhuis JD; Bidlingmaier M; Anderson SM; Evans WS; Wu Z; Strasburger CJ (2002) Impact of Experimental Blockade of Peripheral Growth Hormone (GH) Receptors on the Kinetics of Endogenous and Exogenous GH Removal in Healthy Women and Men. J. Clin. Endocrinol. Metab. 87, 5737–5745. [PubMed: 12466380]

(21). Pfizer, Inc. Somavert (Pegvisomant) [Package Insert]. US Food and Drug Administration website December 2013.

(22). Gaberc-Porekar V; Zore I; Podobnik B; Menart V (2008) Obstacles and Pitfalls in the PEGylation of Therapeutic Proteins. Curr. Opin. Drug Discov. Devel. 11, 242–250.

(23). Payne RW; Murphy BM; Manning MC (2011) Product Development Issues for PEGylated Proteins. Pharm. Dev. Technol. 16, 423–440. [PubMed: 20858059]

(24). Moore DJ; Adi Y; Connock MJ; Bayliss S (2009) Clinical Effectiveness and Cost-Effectiveness of Pegvisomant for the Treatment of Acromegaly: A Systematic Review and Economic Evaluation. BMC Endocr. Disord. 9, 20. [PubMed: 19814797]

(25). Pasut G; Veronese FM (2012) State of the Art in PEGylation: The Great Versatility Achieved after Forty Years of Research. J. Controlled Release 161, 461–472.

(26). Nischan N; Hackenberger CPR (2014) Site-Specific PEGylation of Proteins: Recent Developments. J. Org. Chem. 79, 10727–10733. [PubMed: 25333794]

(27). Dozier JK; Distefano MD (2015) Site-Specific PEGylation of Therapeutic Proteins. Int. J. Mol. Sci. 16, 25831–25864. [PubMed: 26516849]

(28). Wang Y; Wu C (2018) Site-Specific Conjugation of Polymers to Proteins. Biomacromolecules 19, 1804–1825. [PubMed: 29722971]

(29). Belén LH; Rangel-Yagui C, de O; Beltrán Lissabet JF; Effer B; Lee-Estevez M; Pessoa A; Castillo RL; Farías JG (2019) From Synthesis to Characterization of Site-Selective PEGylated Proteins. Front. Pharmacol. 10.

(30). Wu L; Ho SV; Wang W; Gao J; Zhang G; Su Z; Hu T (2013) N-Terminal Mono-PEGylation of Growth Hormone Antagonist: Correlation of PEG Size and Pharmacodynamic Behavior. Int. J. Pharm. 453, 533–540. [PubMed: 23796830]

(31). Ravasco JMJM; Faustino H; Trindade A; Gois PMP (2019) Bioconjugation with Maleimides: A Useful Tool for Chemical Biology. Chem. – Eur. J. 25, 43–59. [PubMed: 30095185]

(32). Gunnoo SB; Madder A (2016) Chemical Protein Modification through Cysteine. ChemBioChem 17, 529–553. [PubMed: 26789551]

(33). Cox GN; Rosendahl MS; Chlipala EA; Smith DJ; Carlson SJ; Doherty DH (2007) A Long-Acting, Mono-PEGylated Human Growth Hormone Analog Is a Potent Stimulator of Weight Gain and Bone Growth in Hypophysectomized Rats. Endocrinology 148, 1590–1597. [PubMed: 17234711]

(34). Wang Y; Langley RJ; Tamshen K; Harms J; Maynard HD; Jamieson SMF; Perry JK (2020) Enhanced Bioactivity of a Human GHR Antagonist by Solid-Phase Site-Specific PEGylation. Unpubl. Manuscipt.

(35). Dumas A; Lercher L; D. Spicer C; G. Davis B (2015) Designing Logical Codon Reassignment – Expanding the Chemistry in Biology. Chem. Sci. 6, 50–69. [PubMed: 28553457]

(36). Cho H; Daniel T; Buechler YJ; Litzinger DC; Maio Z; Putnam A-MH; Kraynov VS; Sim B-C; Bussell S; Javahishvili T; et al. (2011) Optimized Clinical Performance of Growth Hormone with an Expanded Genetic Code. Proc. Natl. Acad. Sci. 108, 9060–9065. [PubMed: 21576502]

(37). Wu L; Chen J; Wu Y; Zhang B; Cai X; Zhang Z; Wang Y; Si L; Xu H; Zheng Y; et al. (2017) Precise and Combinatorial PEGylation Generates a Low-Immunogenic and Stable Form of Human Growth Hormone. J. Controlled Release 249, 84–93.

(38). Deiters A; Schultz PG (2005) In Vivo Incorporation of an Alkyne into Proteins in Escherichia Coli. Bioorg. Med. Chem. Lett. 15, 1521–1524. [PubMed: 15713420]

(39). Bundy BC; Swartz JR (2010) Site-Specific Incorporation of p-Propargyloxyphenylalanine in a Cell-Free Environment for Direct Protein−Protein Click Conjugation. Bioconjug. Chem. 21, 255–263. [PubMed: 20099875]

(40). Miyake-Stoner SJ; Miller AM; Hammill JT; Peeler JC; Hess KR; Mehl RA; Brewer SH (2009) Probing Protein Folding Using Site-Specifically Encoded Unnatural Amino Acids as FRET Donors with Tryptophan. Biochemistry 48, 5953–5962. [PubMed: 19492814]

(41). Hammill JT; Miyake-Stoner S; Hazen JL; Jackson JC; Mehl RA (2007) Preparation of Site-Specifically Labeled Fluorinated Proteins for 19 F-NMR Structural Characterization. Nat. Protoc. 2, 2601–2607. [PubMed: 17948003]

(42). Wang Y; Langley RJ; Tamshen K; Jamieson SM; Lu M; Maynard HD; Perry JK (2020) Long-Acting Human Growth Hormone Receptor Antagonists Produced in E. Coli and Conjugated with Polyethylene Glycol. Bioconjug. Chem. 31, 1651–1660. [PubMed: 32423203]

(43). Conway-Campbell BL; Brooks AJ; Robinson PJ; Perani M; Waters MJ (2008) The Extracellular Domain of the Growth Hormone Receptor Interacts with Coactivator Activator to Promote Cell Proliferation. Mol. Endocrinol. 22, 2190–2202. [PubMed: 18635665]

(44). Presolski SI; Hong VP; Finn MG (2011) Copper-Catalyzed Azide–Alkyne Click Chemistry for Bioconjugation. Curr. Protoc. Chem. Biol. 3, 153–162. [PubMed: 22844652]

(45). Nairn NW; Shanebeck KD; Wang A; Graddis TJ; VanBrunt MP; Thornton KC; Grabstein K (2012) Development of Copper-Catalyzed Azide–Alkyne Cycloaddition for Increased in Vivo Efficacy of Interferon β−1b by Site-Specific PEGylation. Bioconjug. Chem. 23, 2087–2097. [PubMed: 22988919]

(46). Malyala P; Singh M (2008) Endotoxin Limits in Formulations for Preclinical Research. J. Pharm. Sci. 97, 2041–2044. [PubMed: 17847072]

(47). Kenry Liu, B. (2019) Bio-Orthogonal Click Chemistry for In Vivo Bioimaging. Trends Chem. 1, 763–778.

(48). Kim E; Koo H (2019) Biomedical Applications of Copper-Free Click Chemistry: In Vitro, in Vivo, and Ex Vivo. Chem. Sci. 10, 7835–7851. [PubMed: 31762967]

(49). Alley SC; Benjamin DR; Jeffrey SC; Okeley NM; Meyer DL; Sanderson RJ; Senter PD (2008) Contribution of Linker Stability to the Activities of Anticancer Immunoconjugates. Bioconjug. Chem. 19, 759–765. [PubMed: 18314937]

(50). Lyon RP; Setter JR; Bovee TD; Doronina SO; Hunter JH; Anderson ME; Balasubramanian CL; Duniho SM; Leiske CI; Li F; Senter PD (2014) Self-Hydrolyzing Maleimides Improve the Stability and Pharmacological Properties of Antibody-Drug Conjugates. Nat. Biotechnol. 32, 1059–1062. [PubMed: 25194818]

(51). Peschke B; Zundel M; Bak S; Clausen TR; Blume N; Pedersen A; Zaragoza F; Madsen K (2007) C-Terminally PEGylated HGH-Derivatives. Bioorg. Med. Chem. 15, 4382–4395. [PubMed: 17482822]

(52). Tropea JE; Cherry S; Waugh DS Expression and Purification of Soluble His6-Tagged TEV Protease. In High Throughput Protein Expression and Purification: Methods and Protocols; Doyle SA, Ed.; Methods in Molecular Biology; Humana Press: Totowa, NJ, 2009; pp 297–307.

(53). Rappsilber J; Mann M; Ishihama Y (2007) Protocol for Micro-Purification, Enrichment, Pre-Fractionation and Storage of Peptides for Proteomics Using StageTips. Nat. Protoc. 2, 1896–1906. [PubMed: 17703201]

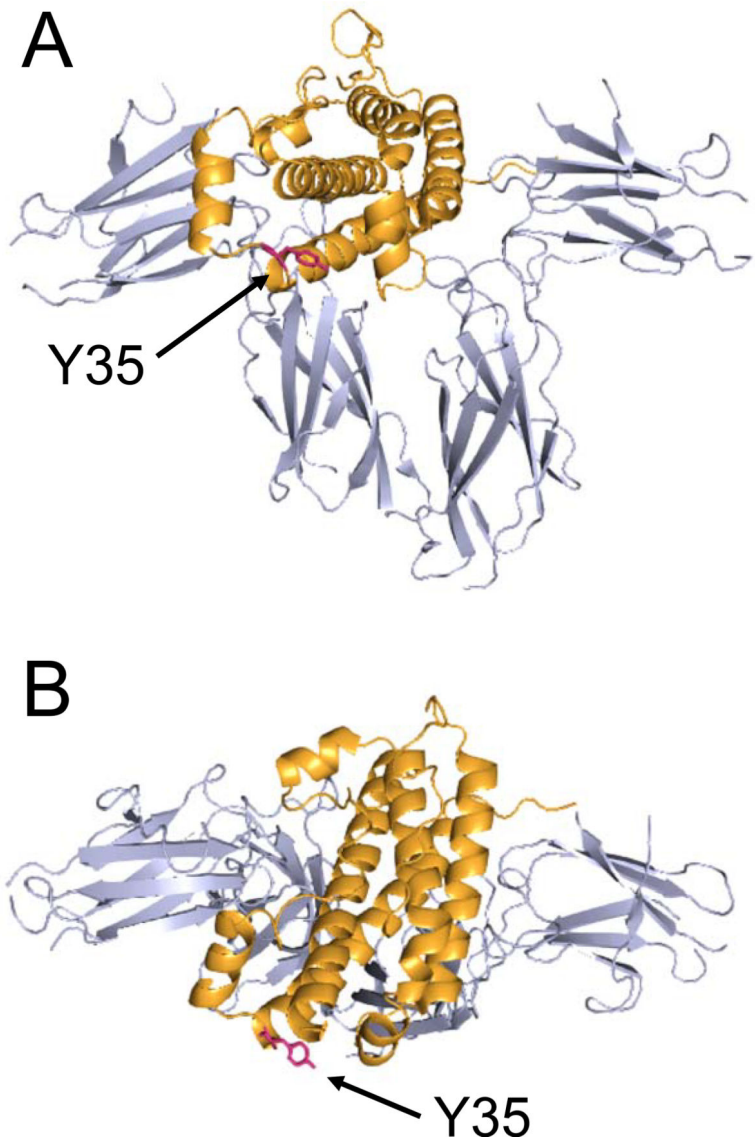

Figure 1.

Schematic of GH (orange) bound to two GHR (grey) with indicated residue Y35 (red) as viewed side-on (A) and top-down (B). PyMol v.1.8.6.0 was used to render the reported crystal structure (PDB 3HHR).[15]

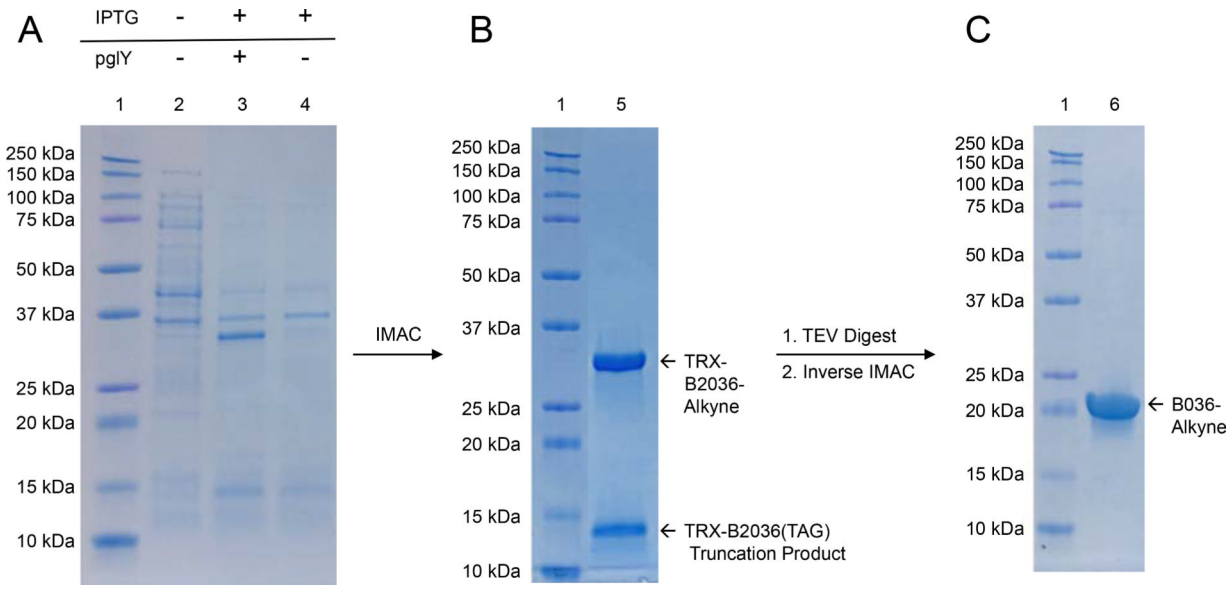

Figure 2.

Expression and purification of B2036-Alkyne evaluated by SDS-PAGE with Coomassie staining. (A) OD_{600} normalized crude cell lysates were evaluated for full-length expression of TRX-B2036-Y35pglY in the presence or absence of isopropyl-β-D-thiogalactopyranoside (IPTG) and propargyl tyrosine (pglY). (B) TRX-B2036-Alkyne purified by immobilized metal affinity chromatography (IMAC). (C) Pure B2036-Alkyne following Tobacco Etch Virus (TEV) protease digestion and inverse IMAC. Lanes were loaded as follows: lane 1: protein standards, lane 2: crude cell lysate without IPTG and without pglY, lane 3: crude cell lysate with both IPTG and pglY, lane 4: crude cell lysate with IPTG and without pglY, lane 5: purified TRX-B2036-Alkyne with TRX-B2036 truncation product as indicated, lane 6: pure B2036-Alkyne; loading was normalized to 1.00 OD_{600}/ml for lanes 2–4; expected TRX-B2036-Alkyne MW = 33 kDa and truncation product = 15 kDa.

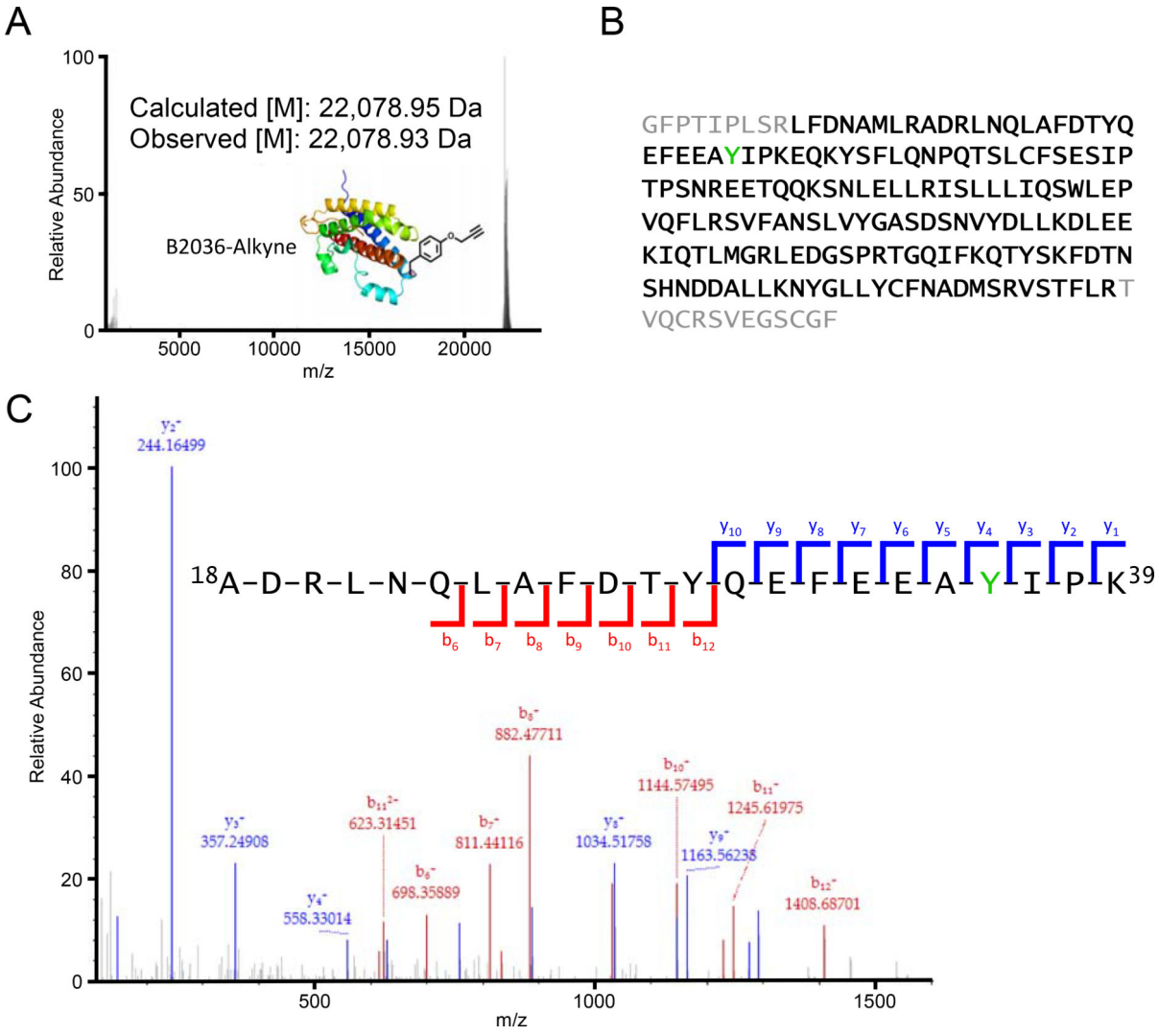

Figure 3.

Mass spectral analysis of B2036-Alkyne. (A) Deconvoluted intact high-resolution mass spectrum of B2036-Alkyne. (B) Sequence coverage map of B2036-Alkyne was determined following digestion of the purified protein with trypsin and identification of the resulting peptides via LC/ESI/MS/MS. Sequence coverage was determined to be 88.5% (black bolded text) with 100% sequence match and includes coverage of the incorporated noncanonical amino acid propargyl tyrosine (green). (C) Sample tandem mass spectrum of the peptide ADRLNQLAFDTYQEFEEA(pglY)IPK with m/z = 2699.30 in LC/ESI/MS analysis following trypsin digestion of B2036-Alkyne with assigned y- and b- series ions (blue and red, respectively).

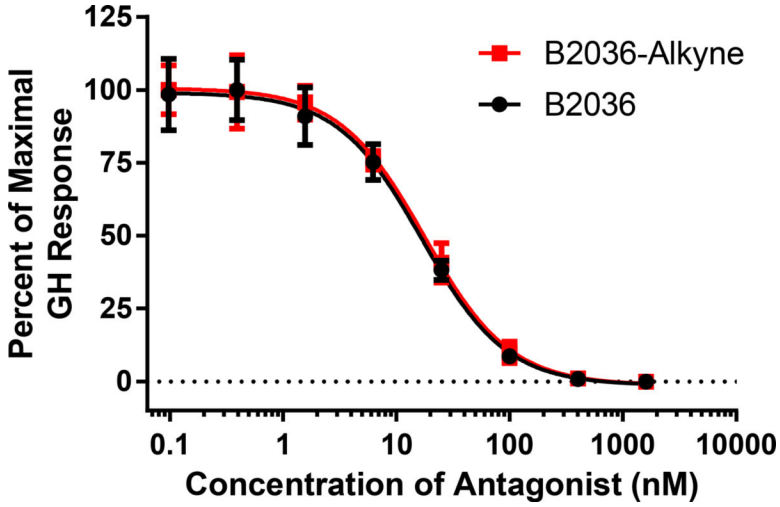

Figure 4.

Inhibitory bioactivity dose response curves of B2036 (black) and B2036-Alkyne (red) with IC_{50} values of 16.8 and 17.7 nM, with 95% confidence intervals (95% CI) of 14.4–19.6 and 15.5–20.2 nM, respectively, in Ba/F3-GHR cells. No significant difference in bioactivity was observed between B2036 and B2036-Alkyne following comparison by Student's t-test ($p > 0.05$). Data is expressed as mean values with 95% CI of two individual experiments.

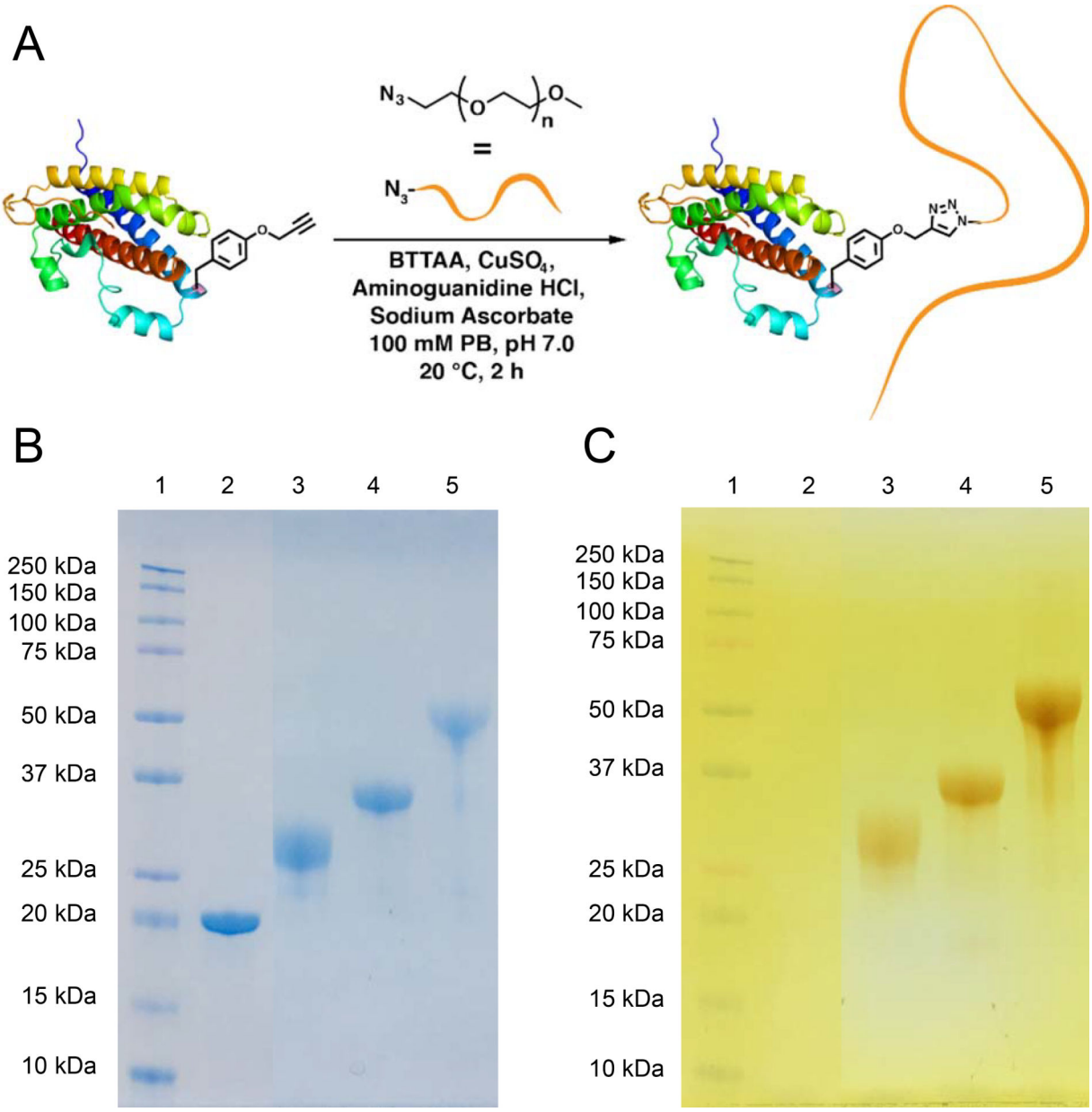

Figure 5.

Site-specific PEGylation of B2036-Alkyne. (A) Scheme of conjugation of PEG-azide to B2036-Alkyne via CuAAC. SDS-PAGE of purified site-specific B2036-PEG conjugates stained with (B) Coomassie to visualize protein and (C) 0.1 M iodine to visualize PEG. Lane 1: protein standards; lane 2: B2036-Alkyne; lane 3: B2036–5k mPEG; lane 4: B2036–10k mPEG; lane 5: B2036–20k mPEG.

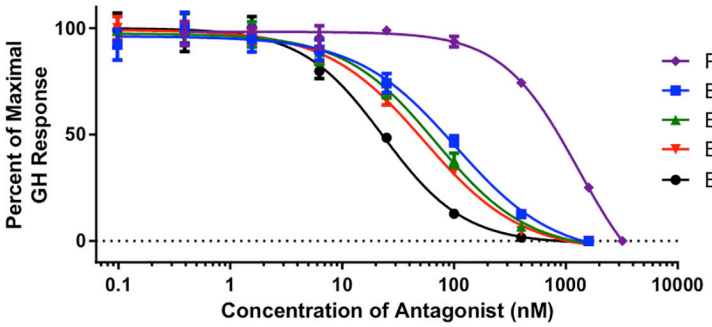

GHR Antagonist	IC_{50} (nM)	95% CI (nM)
Pegvisomant	1289	906.0-1833
B2036-20k mPEG	103.3	81.2-131.3
B2036-10k mPEG	68.8	58.0-81.7
B2036-5k mPEG	54.0	47.8-60.9
B2036-Alkyne	17.7	15.5-20.2

Figure 6.

Inhibitory bioactivity dose response curves of B2036-Alkyne, site-specifically PEGylated B2036, and the multi-PEGylated pegvisomant in Ba/F3-GHR cells. The IC_{50} values for each GHR antagonist are displayed in the table to the right. All IC_{50} values were determined to be statistically different from each other ($p < 0.05$) except for B2036–5k mPEG and B2036–10k mPEG ($p > 0.05$) using one-way ANOVA with post-hoc analyses (Tukey's multiple comparisons test). Data is expressed as means with 95% confidence intervals (95% CI) of two individual experiments.